PROC. OF JSCE,
NO. 220, DEC. 1973

POSTBUCKLING ANALYSIS OF RECTANGULAR PANELS WITH FLANGES BEHAVING ELASTO-PLASTICALLY

*By Eiichi WATANABE**

ABSTRACT

With the advance of engineering know-how, high strength steel, and the fabrication of steel structures, there has been a tendency of steel structures being designed and fabricated thinner and more flexible.

However, incessant accidents and collapses of such structures have made the engineers of the world reconsider the ultimate strength of the structures and called for establishing more accurate design codes.

One of the simplest thin-walled structures would be a plate girder that consists of a webplate, flanges, and stiffeners.

Even a precise investigation on the behavior of plate girder panels will reveal complicated and rather random performances due to the nature of the parametric loading and imperfections.

In this paper, an application of perturbation method is discussed to take into account the stress redistribution and the change of various rigidities due to the large deflection of webplates and the elasto-plastic behavior of flanges. Special attention is paid on the effect of residual stress of flanges upon the load carrying capacity of girders.

The numerical computation was performed by means of finite differences to take into account many boundary conditions solving for unknown displacements.

The analytical results were compared with those from the experiments conducted at other institutions.

As a result of the analysis, it was found that the existence of large residual stress of flanges is not desirable for the load carrying capacity of plate girders, and that the postbuckling performance may significantly differ depending on the individual properties of the panels.

* Ph.D., Assistant Professor of Civil Engineering, Kyoto University.

1. INTRODUCTION

In this paper, an attempt was made to find the effects of the residual stress of flanges, initial curvatures of webplate, rigidities of flanges upon the load carrying capacity of plate girder panels undergoing finite deflection subjected to bending, shear, or the combination of the two.

Since considerable residual stress exists inevitably in the flanges, the finite deflection analysis of webplates must also take into account the elasto-plastic behavior of the flanges due to the residual stress, particularly when the panel is subjected to pure bending. The plastification of the flanges would reduce the flexural and torsional rigidities as well, resulting in less load carrying capacity of girders.

This study aims at finding some of the unstable performances of plate girder panels when the ultimate loads approach in excess of the linear buckling loads of webplates.

2. IDEALIZATION AND ASSUMPTIONS

The assumptions made herein are as follows:

1. The panel can be simulated by a rectangular thin plate and four beams representing the webplate, two flanges and two vertical stiffeners, respectively as is shown in Fig. 1.[1),2)] Moreover, these beams are assumed to possess negligibly small cross sectional dimension; however, they have concentrated cross sectional areas and rigi-

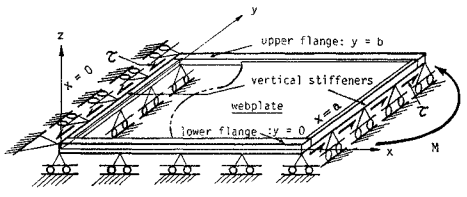

Fig. 1 Mechanical Model of Rectangular Plate Girder Panel.

dities.

2. The webplate and stiffeners remain elastic; however, the flanges are assumed to consist of perfectly elasto-plastic material.

3. The load acts in the plane of webplate. The loading is a general combination of bending moment and shearing force.

4. The residual stresses in the webplate are relatively small; while those in the flanges are of triangular distribution and their magnitude is not limited to small value. Thus, a discontinuity is allowed in the distribution of residual stress between flanges and webplate. The change of flange stress due to the increment of load is shown in Fig. 2.[3),4)]

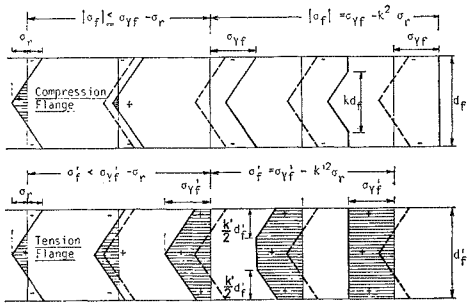

Fig. 2 Mean Flange Stresses σ_f, σ'_f Corresponding to Various Phases of Loading.

5. The in-plane displacement components before loading can be neglected; however, the initial deflection of webplate is taken into account being represented by appropriate trigonometric series.

6. The behavior of webplates obeys the large deflection equation of plates. Lagrangean strain is used.

3. BASIC RELATIONS

Let the column vectors of two-dimensional strain and stress components of the webplate for the in-plane and out-of-plane be designated by $\underline{\bar{\varepsilon}}$, $\underline{\bar{\sigma}}$ and $\underline{\bar{\varepsilon}}_b$, $\underline{\bar{\sigma}}_b$, respectively. Furthermore, let $\underline{u}$ designate a column vector of the in-plane displacement, subscript $_0$ refer to the initial state in general, and subscript t imply transposing matrices; then, the following relations hold:

$$(\underline{\bar{\sigma}}, \underline{\sigma}_b)=(\underline{\bar{\sigma}}_0, \underline{\sigma}_{b0})+(d\underline{\bar{\sigma}}, d\underline{\sigma}_b)$$
$$=(\underline{\bar{\sigma}}_0, \underline{\sigma}_{b0})+\boldsymbol{S}(d\underline{\bar{\varepsilon}}, d\underline{\varepsilon}_b)$$
$$(\underline{\bar{\varepsilon}}, \underline{\varepsilon}_b)=(\underline{\bar{\varepsilon}}_0, \underline{\varepsilon}_{b0})+(d\underline{\bar{\varepsilon}}, d\underline{\varepsilon}_b)$$
$$\underline{\sigma}^t=(\sigma_x, \sigma_y, \tau_{xy}); \quad \underline{\varepsilon}^t=(\varepsilon_x, \varepsilon_y, \gamma_{xy}); \quad \}$$

$$\boldsymbol{S}=\frac{E}{1-\nu^2}\begin{bmatrix} 1 & \nu & 0 \\ \nu & 1 & 0 \\ 0 & 0 & \frac{1}{2}(1-\nu) \end{bmatrix} \quad \Big\} \cdots(1)$$

$$(d\underline{\bar{\varepsilon}}, d\varepsilon_b)=\Big(\boldsymbol{R}^t d\underline{u}+(\boldsymbol{R}^t\boldsymbol{w}_0)(\boldsymbol{T}dw)$$
$$+\frac{1}{2}(\boldsymbol{R}^t dw)(\boldsymbol{T}dw), \ -z\boldsymbol{R}^t\boldsymbol{T}dw\Big)$$

$$\boldsymbol{R}=\begin{bmatrix} D_x & 0 & D_y \\ 0 & D_y & D_x \end{bmatrix}; \quad \boldsymbol{T}=\begin{Bmatrix} D_x \\ D_y \end{Bmatrix};$$
$$\boldsymbol{w}=\begin{bmatrix} w & 0 \\ 0 & w \end{bmatrix}$$

$$\underline{u}=\underline{u}_0+d\underline{u}=\begin{Bmatrix} u \\ v \end{Bmatrix};$$
$$w=w_0+dw=w^{(0)}+w^*+dw$$

where w_0, $w^{(0)}$, and w^* refer to the total initial deflection, initial elastic deflection, and initial inelastic deflection due to some causes other than loading. Furthermore, D_x and D_y, or $,_x$ and $,_y$ imply the differentiation with respect to the coordinates x, and y.

Furthermore, the relationship between the average stress and the in-plane displacement component u along the compression flange, according to Fig. 2, is expressed by the following equation:

$$\left.\begin{array}{l} \sigma_f=Eu_{,x} \\ \qquad \text{when} \quad |\sigma_f|<\sigma_{Yf}-\sigma_r, \\ \text{and} \\ \sigma_f=-(1-k^2\zeta_f)\sigma_{Yf} \\ \qquad \text{when} \quad \sigma_{Yf}-\sigma_r \leqq |\sigma_f| \leqq \sigma_{Yf} \end{array}\right\} \cdots(2)$$

where

$$k=\frac{1}{2}\left(1+\frac{1}{\zeta_f}-\frac{1}{\alpha_f\zeta_f}u_{,x}\right):$$

ratio of elastic cross section, and

$$\alpha_f=\sigma_{Yf}/E; \quad \zeta_f=\sigma_r/\sigma_{Yf}.$$

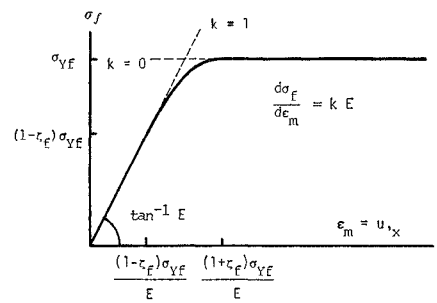

Fig. 3 Relationship between the Average Stress and Strain of the Compression Flange.

The relationship between the average stress and strain is illustrated in Fig. 3. Similar relationship can be obtained along the tension flange. Using the expression of k, various rigidities can be expressed in the elasto-plastic range.

The residual stress distribution in the webplate considered is given in Fig. 4 besides with its mathematical representation.[5] However, its magnitude is considered to be relatively small. Consequently, a discontinuity in the residual stress distribution exists at the lines where the webplate and flanges intersect.

The initial deflection is one of the least known quantities. Fig. 5 presents sketches of some test

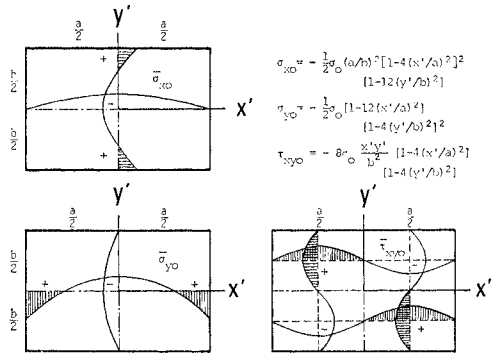

Fig. 4. Residual Stress Distributions in Webplate.

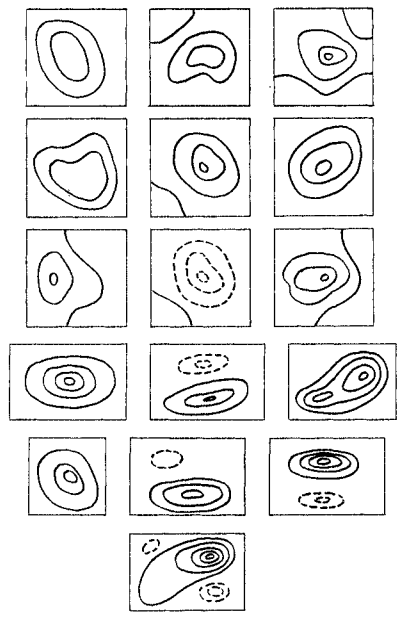

Fig. 5 Sketches of Initial Deflections of Webplate.

girder panels.[6),7),8)] It is seen that these patterns are quite complex and by no means systematic. Even so, it might be reasonable to think that the most common deflectional pattern is of one half wave in both x- and y-directions; therefore, the following representation of the initial deflectional pattern is adopted in this paper:

$$\left.\begin{aligned} w_0(x,\,y)&=\frac{1}{4}(w_0)_{\max}\left(1-\cos\frac{2m\pi x}{a}\right)\\ &\quad\times\left(1-\cos\frac{2n\pi y}{b}\right)\\ \text{or}&\\ w_0(x,\,y)&=(w_0)_{\max}\sin\frac{m\pi x}{a}\cdot\sin\frac{n\pi y}{b}\end{aligned}\right\}\quad\cdots\cdots(3)$$

Using the expressions of Eq. (1), the equations of equilibrium of the webplate can be written in the following form:

$$\left.\begin{aligned} &\boldsymbol{RSR}^t d\underline{u}+\boldsymbol{RS}(\boldsymbol{R}^t\boldsymbol{w}_0)(\boldsymbol{T}dw)\\ &\qquad+\frac{1}{2}\boldsymbol{RS}(\boldsymbol{R}^t d\boldsymbol{w})(\boldsymbol{T}dw)=0\\ \text{in the plane of webplate, and}&\\ &\frac{D}{h}\nabla^4 dw=[\boldsymbol{T}^t\boldsymbol{R}(w_0+dw)]\\ &\qquad\times\boldsymbol{S}\left[\boldsymbol{R}^t d\underline{u}+(\boldsymbol{R}^t\boldsymbol{w}_0)(\boldsymbol{T}dw)\right.\\ &\qquad\left.+\frac{1}{2}(\boldsymbol{R}^t d\boldsymbol{w})(\boldsymbol{T}dw)\right]+(\boldsymbol{T}^t\boldsymbol{R}dw)\bar{\sigma}_0\end{aligned}\right\}\quad\cdots\cdots(4)$$

for the plate-bending; where D, h, and ∇^4 refer to the flexural rigidity of plate, thickness of the webplate, and the biharmonic operator.

Let subscripts f, f', s, and s' denote the compression flange, tension flange, left stiffener, and right stiffener, respectively. Furthermore, let σ denote the average stress in each member in general, and A, EI, Ei, GJ, I_p, and σ_Y denote, in general, the cross sectional area, flexural rigidity about the strong axis, flexural rigidity about the weak axis, torsional rigidity, polar moment of inertia, and the yielding strength of steel, respectively.

Then, the boundary conditions can be stated by the following equations:

$$\left.\begin{aligned} &x=0\\ &\quad w_e=0;\quad GJ_s w_{e'xyy}=D(D_{xx}+\nu D_{yy})w_e;\\ &\quad u=0;\quad A_s\sigma_{s'y}+h\bar{\tau}_{xy}=h\tau\\ \text{where}&\\ &\quad w_e=w^{(0)}+dw\end{aligned}\right\}\quad\cdots\cdots(5)$$

$x=a$

$$\left.\begin{aligned} &w_e=0; \quad GJ'_s w_{e,xyy}=-D(D_{xx}+\nu D_{yy})w_e; \\ &u_{,yy}=0; \quad A'_s\sigma_{s,y}-h\tau_{xy}=-h\tau \end{aligned}\right\} \quad \cdots\cdots(6)$$

$y=0$

$$\left.\begin{aligned} &w_e=0; \quad K'GJ'_f w_{e,xxy}=D(D_{yy}+\nu D_{xx})w_e; \\ &A'_f\sigma'_{f,x}+h\bar{\tau}_{xy}=0; \\ &h\bar{\sigma}_y+A'_f D_x(\sigma'_f v_{,x})=k'Ei'_f v_{,xxxx} \end{aligned}\right\} \quad \cdots\cdots(7)$$

where K' is an equivalent torsional rigidity ratio defined by Total Strain Theory in the following form:[9]

$$K'=k'+\frac{1+\nu}{3\zeta'_f}\log_e\frac{1}{1+\nu}[1+\nu+3\zeta'_f(1-k')];$$

$$\zeta'_f=\sigma'_\tau/\sigma'_{Yf}$$

$y=b$

$$\left.\begin{aligned} &D[D_{yyy}+(2-\nu)D_{xxy}]w_e+A_f\sigma_f w_{,xx} \\ &=k^3 EI_f w_{e,xxxx} \\ &KGJ_f w_{e,xxy}+D(D_{yy}+\nu D_{xx})w_e \\ &=I_p\left(\sigma_{Yf}-\frac{k^4}{2}\sigma_\tau\right)w_{,xxy}[|\sigma_f|\geqq\sigma_{Yf}-\sigma_\tau] \\ &=I_p\left(|\sigma_f|+\frac{1}{2}\sigma_\tau\right)w_{,xxy}[|\sigma_f|<\sigma_{Yf}-\sigma_\tau] \\ &A_f\sigma_{f,x}-h\bar{\tau}_{xy}=0 \\ &-h\bar{\sigma}_y+A_f D_x(\sigma_f v_{,x})=kEi_f v_{,xxxx} \end{aligned}\right\}$$

where

$$K=k+\frac{1+\nu}{3\zeta_f}\log_e\frac{1}{1+\nu}[1+\nu+3\zeta_f(1-k)];$$

$$\sigma_f=\sigma_\tau/\sigma_{Yf} \quad \cdots\cdots(8)$$

Furthermore, the loading conditions are described in the following form:

$x=0$ and $x=a$

$$\left.\begin{aligned} &h\int_0^b \bar{\sigma}_x dy+A_f\sigma_f+A'_f\sigma'_f=0 \\ &h\int_0^b \bar{\sigma}_x y\,dy+bA_f\sigma_f=-M|_{x=0}(-M|_{x=a}) \end{aligned}\right\} \quad \cdots\cdots(9)$$

$y=0$ and $y=b$

$$\left.\begin{aligned} &h\int_0^a \bar{\sigma}_y dx+A_s\sigma_s+A'_s\sigma'_s=0 \\ &h\int_0^a \bar{\sigma}_y x\,dx+aA'_s\sigma'_s=0 \end{aligned}\right\} \quad \cdots\cdots(10)$$

4. APPLICATION OF PERTURBATION THEORY

Recently, nonlinear structural problems have become of great interest. The methods of linearization include the incremental, Newton-Raphson, modified incremental, and perturbation theories.[10),11),12),13),14),15)] The former three are based on the Taylor series expansion of the first order; while the last one is based on that of the second order. For this reason, the perturbation method allows fairly large size of increments; furthermore, it also allows free choice of incremental load or displacement as the perturbation parameter according to the situation.

Let $\underline{u}$ and p designate the displacement vector and the load in general, then, the problem can be generally stated by the following matrix equation:

$$\boldsymbol{K}(\underline{u})\underline{u}=\underline{f}(p,\underline{u}); \quad \underline{u}^t=(u,v,w) \quad \cdots\cdots(11)$$

where $\boldsymbol{K}(\underline{u})$ and $\underline{f}(p,\underline{u})$ refer to integro-differential operator and some function vector, respectively.

Denoting the initial state by subscript $_0$, the following equations can be obtained by considering the variations of $\underline{u}$ and p:

$$\begin{aligned} &\boldsymbol{K}_0\underline{u}_0=\underline{f}_0 \\ &[\boldsymbol{K}_0+\boldsymbol{K}_{,\underline{u}}\underline{u}_0-\underline{f}_{,\underline{u}}]\delta\underline{u} \\ &=\underline{f}_{,p}\delta p+\frac{1}{2}\underline{f}_{,\underline{uu}}\delta\underline{u}\,\delta\underline{u}+\underline{f}_{,\underline{u}p}\delta p\,\delta\underline{u} \\ &\quad -\boldsymbol{K}_{,\underline{u}}\delta\underline{u}\,\delta\underline{u}+\frac{1}{2}\underline{f}_{,pp}\delta p^2-\frac{1}{2}\boldsymbol{K}_{,\underline{uu}}\underline{u}_0\delta\underline{u}\,\delta\underline{u} \\ &\quad +O(\delta^3) \end{aligned} \quad \cdots\cdots(12)$$

Let these variations be expressed by the following series:

$$\left.\begin{aligned} &\delta\underline{u}=\underline{u}^{(1)}\Delta+\underline{u}^{(2)}\Delta^2+O(\Delta^3) \\ &\delta p=p^{(1)}\Delta+p^{(2)}\Delta^2+O(\Delta^3) \end{aligned}\right\} \quad \cdots\cdots(13)$$

Then, the second equation of Eq. (12) can be rewritten for each power of Δ:

$$\begin{aligned} &[\boldsymbol{K}_0+\boldsymbol{K}_{,\underline{u}}\underline{u}_0-\underline{f}_{,\underline{u}}](\underline{u}^{(1)},\underline{u}^{(2)}) \\ &=\underline{f}_{,p}(p^{(1)},p^{(2)})+\frac{1}{2}\underline{f}_{,\underline{uu}}(O,\underline{u}^{(1)}\underline{u}^{(1)}) \\ &\quad +\underline{f}_{,\underline{u}p}(O,p^{(1)}\underline{u}^{(1)})+\frac{1}{2}\underline{f}_{,pp}(O,p^{(1)2}) \\ &\quad -\frac{1}{2}\boldsymbol{K}_{,\underline{uu}}\underline{u}_0(O,\underline{u}^{(1)}u^{(1)})-\boldsymbol{K}_{,\underline{u}}(O,\underline{u}^{(1)}\underline{u}^{(1)}) \end{aligned} \quad \cdots\cdots(14)$$

Appendix A demonstrates some of the perturbed equations. The solution of the problem initiates from solving this linearized zero-order equations and proceeds by solving higher order equations until the highest, 2nd in this study, equations are solved. Thereafter, the initial values such as $\underline{u}_0$, $\boldsymbol{K}_0$, $\boldsymbol{K}_{,\underline{u}}$, $\boldsymbol{K}_{,\underline{uu}}$, $\underline{f}_0$ and $\underline{f}_{,\underline{u}}$ are up-to-dated for each increment of Δ, by assigning the final values in the preceeding step of the loading his-

tory. The complete solution will be obtained by repeating the procedure as mentioned above.

So far, nothing has been mentioned what quantity should be taken for Δ, nor how it should be determined. Considering the first of Eq. (13), it will be seen that $\underline{u}^{(1)}$ implies the tangent value of $\underline{u}$-Δ curve. Thus, the increment of load would be conveniently chosen for Δ unless the above-mentioned tangent value is considerably large, because the load-deflection curves are well investigated by experiments and known to reflect the over-all behavior of the plate girder panels. On the other hand, the increment of deflection at certain point in the panel would be covenientlly taken for Δ when the tangent mentioned formerly exceeds certain value. Thus, the increment of load and the increment of deflection at certain point can be taken alternately during the solution process for the perturbation parameter Δ.

The remaining problem would be how to control the value of Δ. It would be reasonable to think that this value must be smaller whenever the system undergoes significant change, for example, near at the linear buckling load of the webplate, and in the elasto-plastic range of flanges. Besides for the gradual plastification of flanges, this value can be conveniently controlled by considering equal line segment of load-deflection curve at certain point of the webplate. Consider the deflection w_j of point j, and let the scale factor of the deflection be C_s, then, the equal arc length, l, can be determined by the following equation:

$$l=\int_0^{\Delta}\sqrt{1+(w_{j,\varepsilon}/C_s)^2}\,d\varepsilon$$
$$=\frac{2q\Delta+p}{4q}\sqrt{4q^2\Delta^2+4pq\Delta+p^2+1}$$
$$+\frac{1}{4|q|}\log_e\left|\frac{\sqrt{4q^2\Delta^2+4pq\Delta+p^2+1}}{\sqrt{1+p^2}}\right.$$
$$\left.\frac{+2|q|\Delta+p\ \mathrm{sign}\,(q)}{+p\ \mathrm{sign}\,(q)}\right|-\frac{p}{4q}\sqrt{1+p^2}$$
$$\cdots\cdots(15)$$

where

$$p=w_j^{(1)}/C_s \quad \text{and} \quad q=w_j^{(2)}/C_s\,.$$

When flanges are in elasto-plastic range, l should be determined so that each new plastification of point can be detected.

It should be noted however that the perturbation theory is applicable only when the system undergoes relatively gradual change because the oncoming state of the system can be predicted merely by the preceding state. For instance, the abrupt increment of the deflection of the webplate at or near the theoretical buckling load of the webplate can be predicted by the theory because of the existence of the initial deflection.

5. NUMERICAL COMPUTATION BY MEANS OF FINITE DIFFERENCES

The analytical solution of the equations in Eqs. (4) through (10) is practically impossible. For this reason, the numerical solution by means of finite differences is applied in this study.

The numerical solution consists in the successful evaluation of the displacement vectors $\underline{u}(x, y)$ as the load increases. Fig. 6 illustrates three mesh point systems corresponding to the displacement components u, v, and w. According to the figure, the number of the total displacement components n, the in-plane displacement components n_i, the components in x-direction n_u, the components in y-direction n_v, and the out-of-plane displacement components n_w, are given respectively by:

$$n=3N^2+9N-11;\quad n_i=n_u+n_v=2N^2+7N-3$$
$$n_u=N^2+3N-2;\quad n_v=N^2+4N-1;$$
$$n_w=N^2+2N-8\,.$$

On the other hand, all of the equations, namely, the equations of equilibrium, Eqs. (A-1) and

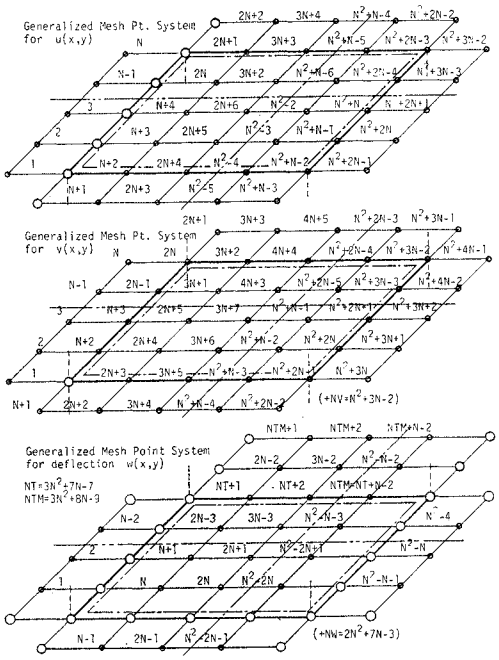

Fig. 6 Generalized Mesh Point System for $u(x, y)$, $v(x, y)$ and $w(x, y)$.

(A-2), and the necessary boundary conditions such as Eqs. (A-5) and (A-6) can be written on the basis of the mesh point systems chosen.

Throhgh the finite difference operation, all of the equations, represented generally by Eq. (14), can be algebraically written in the similar matrix form. However, now the displacement vector $\underline{u}$ is such that

$\underline{u}^t=(u_1, u_2, \cdots, u_{n_u}, v_1, v_2, \cdots, v_{n_v}, w_1, w_2, \cdots, w_{n_w})$

and $K, \underline{u}\underline{u}_0$, $K, \underline{uu}\underline{u}^{(1)}\underline{u}^{(1)}$, and $\underline{f}, \underline{u}$ are n by n matrices; while $\underline{u}_0$, $\underline{u}^{(i)}$, and $\underline{f}, \underline{p}$ are vectors of order n.

This matrix equation indicates that it is a set of linear algebraic equations with respect to $\underline{u}^{(1)}$ and $\underline{u}^{(2)}$, also that the results of the first order equations are substituted to obtain the second order solution, $\underline{u}^{(2)}$. Furthermore, it also implies that $p^{(1)}$ and $p^{(2)}$ can be regarded as unknowns when the increment dw_p of deflection w_p of a particular point is chosen for the perturbation parameter, Δ. In that case, $w_p^{(1)}$ and $w_p^{(2)}$ are considered to be 1, and 0, respectively.

6. TORSIONAL BUCKLING OF COMPRESSION FLANGE —SIMPLIFIED MODEL—

If the cross section of plate girder is replaced by the model shown in Fig. 7, the equation of equilibrium of the compression flange is simply given by the equation:[9]

$$KGJ_f\theta'_{xx}-\left[\int_A|\sigma_f|r^2dA\right](\theta+\theta_0)'_{xx}-K_\theta\theta=0 \quad \cdots\cdots(16)$$

where θ and θ_0 refer to the rotation and the initial rotation of the compression flange, respectively, and

$$K_\theta=\frac{Eh^3}{3b(1-\nu^2)}. \quad \cdots\cdots(17)$$

Furthermore, K refers to the effective torsional

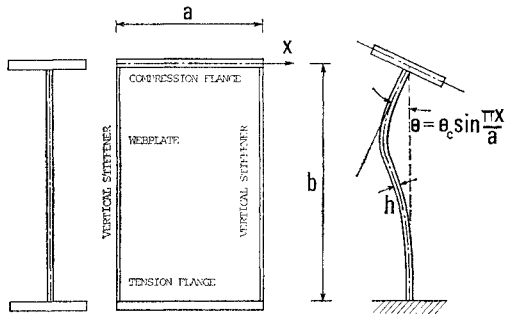

Fig. 7 Simplified Linear Model of Plate Girder Panels.

rigidity ratio of flanges in the elasto-plastic range. In this paper, the following forms of K are used:

$$(1)\quad K=k+\frac{1+\nu}{3\zeta_f}\log_e\frac{1}{1+\nu}[1+\nu+3\zeta_f(1-k)]. \quad \cdots\cdots(18)$$

$$(2)\quad K=k+\frac{1+\nu}{1+\nu+3\zeta_f(1-k)}(1-k). \quad \cdots\cdots(19)$$

Eq. (18) is obtained using Fukomoto's derivation based on the total strain theory;* while Eq. (19) is obtained on the basis of the same theory assuming that the strain of the flange is zero before the loading. Fig. 8 shows the relationship between K and k.

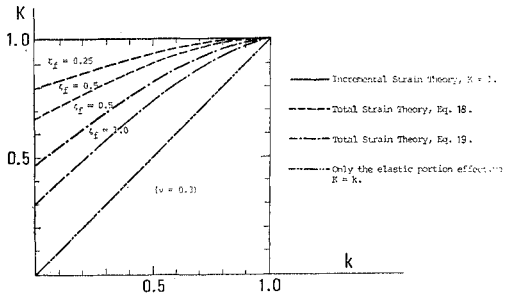

Fig. 8 Relationship between K and k.

Then, the torsional buckling equation will be obtained from Eq. (16) if $\theta_0=0$:

$$\left.\begin{aligned}\beta_f\sqrt{\alpha_f}&=\frac{d_f}{t_f}\sqrt{\sigma_{Yf}/E}\\&=1.24\frac{\sqrt{K+0.289(a/d_f)(h/t_f)^3}}{\sqrt{(1-k^4\zeta_f/2)}}\\&\qquad(\sigma_{Yf}-\sigma_r<\sigma_f\leqq\sigma_{Yf})\\&=1.24\frac{\sqrt{1+0.289(a/d_f)(h/t_f)^3}}{\sqrt{(\sigma_f/\sigma_{Yf}+\zeta_f/2)}}\\&\qquad(\sigma_f\leqq\sigma_{Yf}-\sigma_r)\end{aligned}\right\} \quad \cdots\cdots(20)$$

On the other hand, according to Basler, this relationship can be expressed by the equation:[16]

$$\left.\begin{aligned}\sigma_f/\sigma_{Yf}&=1-0.396(\beta_f\sqrt{\alpha_f}-0.558)^{1.36}\\&\qquad(0.558<\beta_f\sqrt{\alpha_f}<1.753)\\&=1.54/(\beta_f\sqrt{\alpha_f})^2\\&\qquad(1.753\leqq\beta_f\sqrt{\alpha_f})\end{aligned}\right\} \quad \cdots\cdots(21)$$

Fig. 9 illustrates the buckling curves, however, the effect of K_θ is not shown here. If this effect

* Stress-Strain Relationship by Sokolovski:

$d\tau=d\gamma[1/G+3\varepsilon_p/\sigma_Y]$

where ε_p refers to the plastic strain.

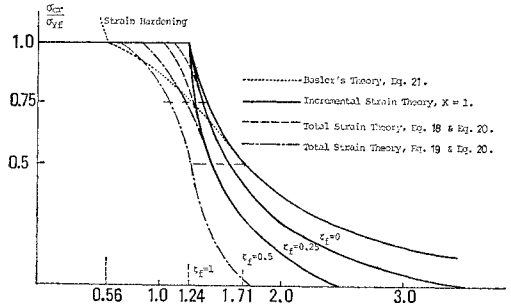

Fig. 9 Torsional Buckling Curves of Compression Flanges.

is to be considered, all of the curves must be shifted to the right to some extent.

7. RESULTS OF COMPUTATIONS

In this paper, emphasis is placed on the behavior of panels subjected to pure bending moment. Two of the tested moment panels will be conveniently amed M-1 and M-2[6], and the details of these panels are listed in Table 1 besides with a shear panel S-1[6] and a panel C-1[7] under combined moment and shear. The parameters of these quoted test panels necessary for the analysis are provided in Table 2.

Table 2 Parameters of Plate Girder Panels

Parameter	M-1	M-2	S-1	C-1
b/a	1.0	1.0	1.0	0.333
a/h	266.7	200.0	266.7	761
d_f/t_f	20.0	20.0	20.0	15.96
d'_f/t'_f	20.0	20.0	20.0	16.06
σ_{Yf}/E	0.001336	0.002381	0.002381	0.001377
σ'_{Yf}/E	0.001336	0.002381	0.002381	0.001377
σ_{Yw}/E	0.001336	0.002381	0.002381	0.001273
$(w_o)_{max}/h$	0.667	0.50	0.667	1.421
$A_f/(ah)$	0.533	0.400	0.533	0.305
$A'_f/(ah)$	0.533	0.400	0.533	0.303
$A_s/(ah)$	0.400	0.300	0.400	0.473
$A'_s/(ah)$	0.400	0.300	0.400	0.473
$J_f/(ah^3)$	1.27	0.533	1.27	1.49
$J'_f/(ah^3)$	1.27	0.533	1.27	1.45
$J_s/(ah^3)$	0.533	0.225	0.533	1.39
$J'_s/(ah^3)$	0.533	0.225	0.533	1.39
$i_f/(ah^3)$	0.32	0.132	0.32	0.37
$i'_f/(ah^3)$	0.32	0.132	0.32	0.37
$I_f/(ah^3)$	126.3	53.3	126.3	94.4
$I_p/(ah^3)$	126.3	53.3	126.3	94.4

Table 1 Description of Plate Girder Panels

Name of Panel (Type of Load)	a [cm]	b [cm]	Webplate h [cm]	Webplate σ_{Yw} [kg/mm²]	Webplate $(w_o)_{max}$* [cm]	Compression Flange t_f [cm]	Compression Flange d_f [cm]	Compression Flange σ_{Yf} [kg/mm²]	Tension Flange t'_f [cm]	Tension Flange d'_f [cm]	Tension Flange σ_{Yf} [kg/mm²]	P_u** [ton]
M-1 (Mom.)	120	120	0.45	28.0	0.30	1.20	24.0	28.0	1.20	24.0	28.0	46.5
S-1 (Shear)	120	120	0.45	50.0	0.30	1.20	24.0	50.0	1.20	24.0	50.0	76.0
M-2 (Mom.)	120	120	0.60	50.0	0.30	1.20	24.0	50.0	1.20	24.0	50.0	96.0
C-1 (M. & S.)	381	127	0.50	26.9	0.71	1.91	30.5	29.0	1.90	30.5	29.0	77.1

* Magnitude of the maximum initial deflection observed during experiment.

** Magnitude of load obtained by experiment: Two-point load for M-1, M-2 and S-1. One-point load for C-1.

Fig. 10 and Fig. 11 demonstrate the effect of the initial deflection upon the load-deflection curves of webplates of M-1 and M-2, respectively. It will be seen that the linear buckling loads of these panels would be approximately 0.16 and 0.13, respectively. Also, it will be seen that the curves tend to converge to each asymptote as the loads increase. Furthermore, it will be quite interesting to note the characteristics of each panel: The load-deflection curves of M-1 are characterized by the typical parabolic portion that is peculiar to the post-buckling performance of plates under uniform compression; while those of M-2 are more complex and show convex portion for larger magnitude of load.

Fig. 12 shows the effect of initial deflection on the load-deflection curve of shear panel S-1. However, in this case the existence of the asymptote is not so clear as previous ones.

Fig. 13 shows some load-deflection characteristics of panel C-1. It will be seen that the deflection at A becomes convex upward; while that at C becomes concave upward. Also, it will be seen that the solutions of different mesh point systems, $N=5$ and $N=7$ are quite close at A.

Figs. 14, 15, 16 and 17 show the effect of residual stress of flanges on the load-deflection curves of M-1 and M-2, of which Figs. 14 and 16 correspond to the initial deflection of sine wave; while Figs. 15 and 17 correspond to that of cosine wave. From these curves, it can be concluded that the deflection of webplate becomes larger as the residual stress increases.

Figs. 18 and 19 show the effect of the residual stress of the flanges upon the relationship between the load and the angle of rotation of the boundary $x=a$. It can be seen that the flexural rigidity of the panel decreases as the residual stress increases.

Figs. 20 and 21 show the effect of the residual

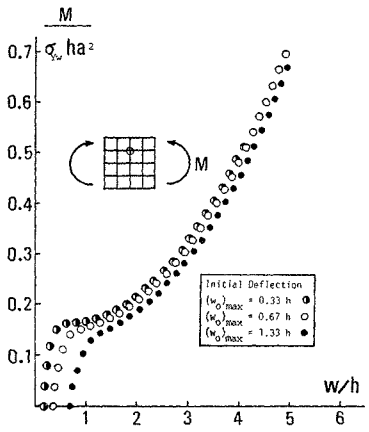

Fig. 10 Effect of Initial Deflection upon the Load-Deflection Relationship: Panel M-1. Initial Deflection: cosine.

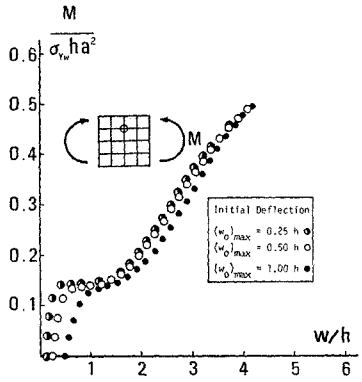

Fig. 11 Effect of Initial Deflection upon the Load-Deflection Relationship: Panel M-2. Initial Deflection: cosine.

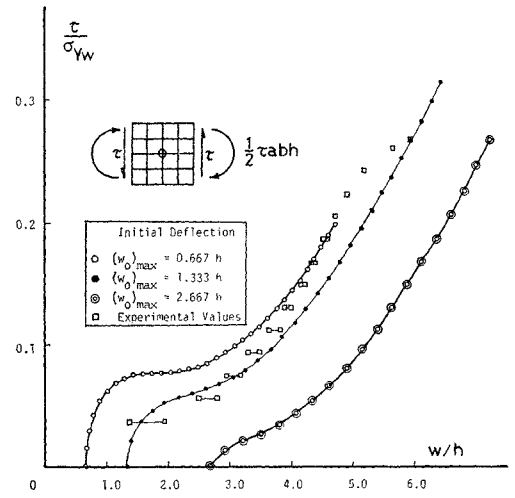

Fig. 12 Effect of Initial Deflection upon the Load-Deflection Relationship: Panel S-1. Initial Deflection: cosine.

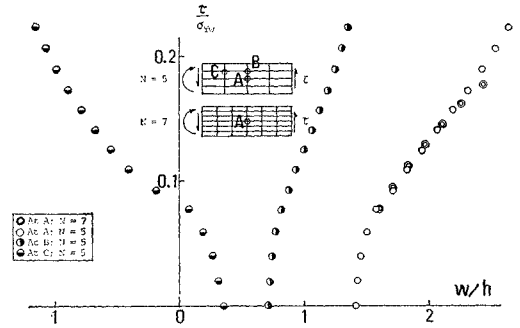

Fig. 13 The Relationship between the Load and Deflections: Panel C-1. Initial Deflection: cosine.

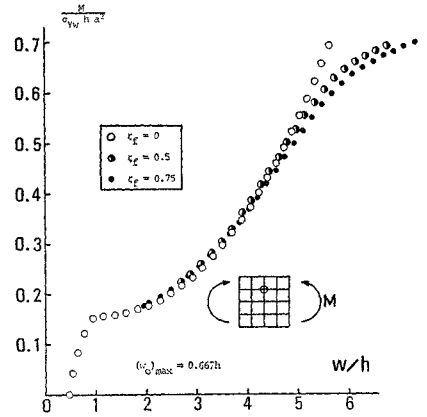

Fig. 14 Effect of Residual Stress of Flanges upon the Load-Deflection Relationship: Panel M-1. Initial Deflection: sine.

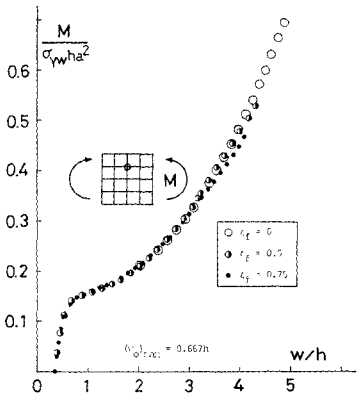

Fig. 15 Effect of Residual Stress of Flanges upon the Load-Deflection Relationship: Panel M-1. Initial Deflection: cosine.

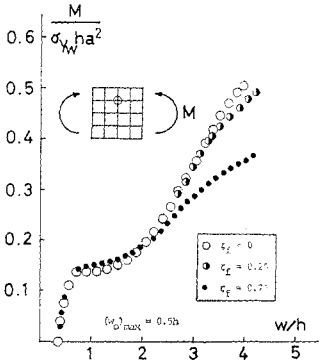

Fig. 16 Effect of Residual Stress of Flanges upon the Load-Deflection Relationship: Panel M-2. Initial Deflection: sine.

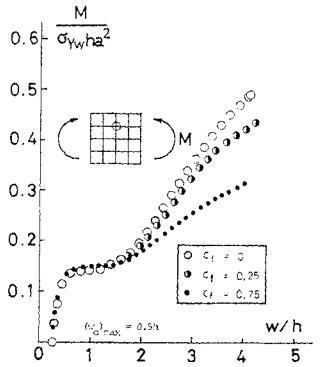

Fig. 17 Effect of Residual Stress of Flanges upon the Load-Deflection Relationship: Panel M-2. Initial Deflection: cosine.

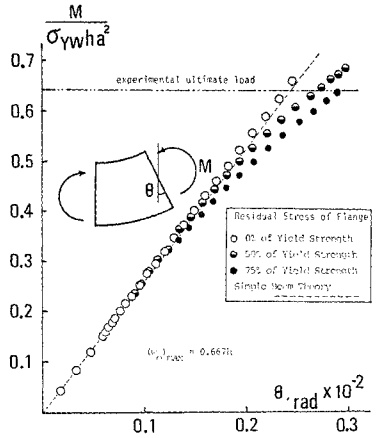

Fig. 18 Effect of Residual Stress of Flanges upon the In-plane Flexural Stiffness of Girder: Panel M-1. Initial Deflection: cosine.

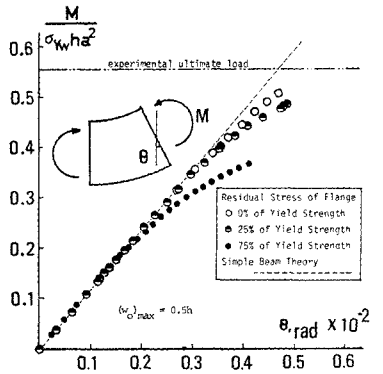

Fig. 19 Effect of Residual Stress of Flanges upon the In-plane Flexural Stiffness of Girder: Panel M-2. Initial Deflection: cosine.

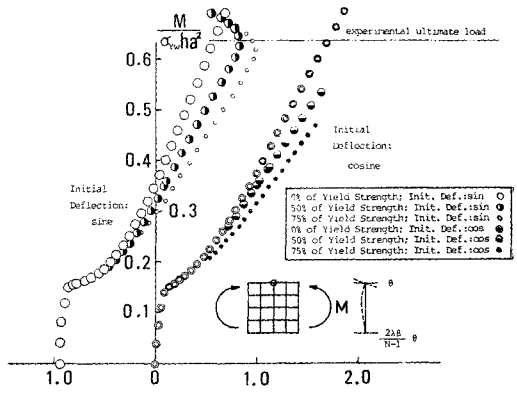

Fig. 20 Effect of Residual Stress of Flanges upon the Twisting of Compression Flange: Panel M-1.

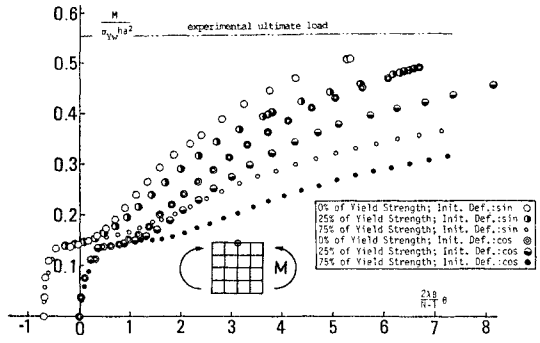

Fig. 21 Effect of Residual Stress of Flanges upon the Twisting of Compression Flange: Panel M-2.

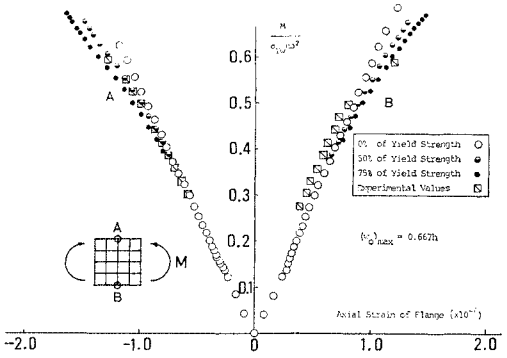

Fig. 22 Effect of Residual Stress of Flanges upon the Strains of Flanges: Panel M-1. Initial Deflection: cosine.

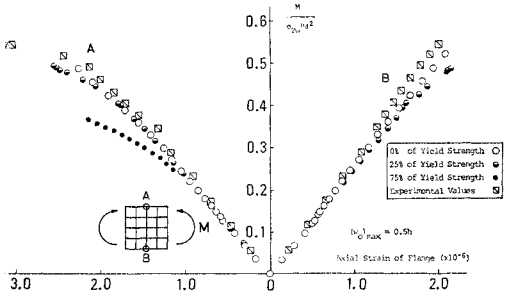

Fig. 23 Effect of Residual Stress of Flanges upon the Strains of Flanges: Panel M-2. Initial Deflection: cosine.

stress of the flanges upon the relationship between the load and the angle of rotation of the compression flange. It will be seen that the rotation becomes larger as the residual stress becomes larger. It is quite interesting to note the abrupt change of the curves at the load of approximately 0.6 of panel M-1 when the initial deflection is of sine wave and the residual stress is more than 50% of the yielding strength. This change is seen to correspond to the sudden increase of the deflection in Fig. 14 and may have something to do with the torsional buckling of the compression flange of M-1.

Figs. 22 and 23 show the effect of the residual stress of the flanges upon the relationship between the load and the flange strains of M-1 and M-2. It will be seen that the strains increase as the residual stress increases, especially in the compression flange.

Fig. 24 shows the change of the distribution of normal stresses $\bar{\sigma}_x\ \sigma_{x1}\ \sigma_{x2}$ of M-1 computed on the mesh $N=7$ as the load increases. It will be seen that the distribution is not linear any more in the compressed portion of the webplate. This is also shown in the load-stress relationship of Fig. 25.

Fig. 26 shows the effect of residual stress of flanges upon the relationship between the flange

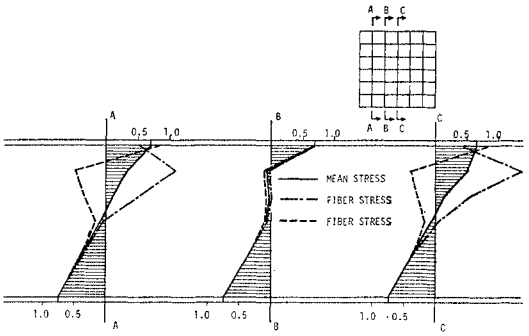

Fig. 24 Distribution of Normal Stresses $\bar{\sigma}_x$, σ_{x1}, σ_{x2} and Flange Stresses σ_f, σ'_f: Test Girder Panel M-1: $\mu=0.167$; $\zeta_f=\zeta'_f=0$; $\Delta=0.541$; $N=7$.

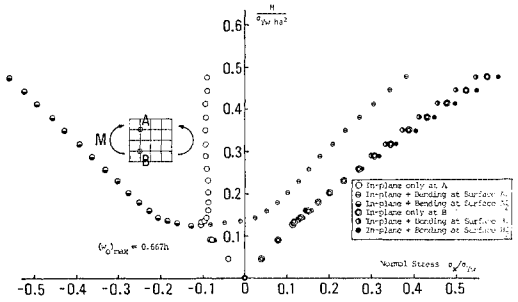

Fig. 25 Relationships between the Load and Normal Stress σ_x: Panel M-1. Initial Deflection: cosine.

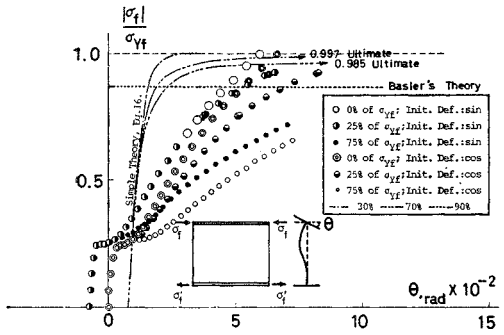

Fig. 26 Effect of Residual Stress of Flanges upon the Twisting of the Compression Flange: Panel M-2. $(w_0)_{max}=0.5$ h or $\theta_e=(\theta_0)_{max}=0.00785$ rad.

stress and the angle of rotation of the compression flange computed on various bases. It is clearly seen that the results from the simple theory, Eq. (16) differ considerably from those of postbuckling analysis near the linear buckling stress of the webplate, since the linear theory does not take into account the buckling of the webplate. Furthermore, it is seen that the torsional buckling will not occur if the flanges have no residual stresses, and the chance of undertaking large rotation of the compression flange increases as the residual stress increases.

8. DISCUSSIONS AND CONCLUSIONS

A set of computer programs were developed in such a way that almost any rectangular panel could be analyzed. If the interval length of load-deflection curve is taken no more than one fourth of the webbuckling load, it was found that no significant propagation errors occur in the perturbation process. As a result, twenty to thirty intervals of loading are found to be necessary to analyze each panel. The necessary CPU time would be approximately little more than ten minutes for $N=5$ $(n=109)$; while it would be more than thirty minutes for $N=7$ $(n=199)$. From this reason, most of the computations were carried out using $N=5$, although it would be desirable to use larger value of N to get more reliable results. A number of convergence checks revealed a fact that as far as the in-plane displacement components are concerned, no significant errors are observed in the case of $N=5$, as shown in Appendix B.

From the results of the proposed analysis, it was found that the postbuckling performance of plate girders may significantly differ depending on their respective properties; furthermore, it was found that the existence of large residual stress in flanges is not desirable for the load carrying capacity of plate girders in bending: It would reduce the in-plane flexural stiffness of plate girders, and result in larger twisting of the compression flanges.

ACKNOWLEDGEMENTS

The author wishes to express appreciation to Professor Yoshikazu Yamada of Kyoto University for his advices and encouragement.

Appreciation is also extended to former graduate student of Kyoto University, Yuhgo Ohtsuki for his help in computer programs and computations.

The computations were performed by FACOM 230-60 at Data Processing Center, Kyoto University.

BIBLIOGRAPHIES

1) Watanabe, E. and Ti-Ta Lee: A method of analysis of webplates with large deflections. Proceedings of Japan Society of Civil Engineers 183: 93-109. 1970.
2) Yamada, Y., E. Watanabe and Y. Ohtsuki: A behavioral analysis of load carrying capacity of plate girders. Proceedings of National Symposium on the Matrix Method for Structural Analysis and Design. Society of Steel Construction of Japan. 455-462. 1971. (in Japanese)
3) Beedle, L. S., J. H. Blackman, P. B. Cooper, G. C. Driscoll, Jr. and W. J. Eney: Structural steel design. Ronald Press Inc., New York. 1964.
4) Rao, N. R. N. and L. Tall: Residual stresses in welded plates. Fritz Engineering Laboratory, Department of Civil Engineering, Lehigh University. Fritz Engineering Laboratory Report: No. 249.7. 1960.
5) Škaloud, M. and J. Donea: Postrical behavior of webs with residual stresses. International Association for Bridges and Structural Engineering Publication 23: 293-320. 1963.
6) Theories and experiments on the load carrying capacity of plate girders. Kansai Research Committee on Bridges, Steel Frames and Welding. Nippon Publishing Company, Inc., Osaka. 1965. (in Japanese)
7) Basler, K., B. T. Yen, J. A. Mueller and B. Thurlimann: Web buckling tests on weld-

ed plate girders. Buttetin Series, Welding Research Council 64. 1960.
8) Patterson, P. J., J. A. Corrado, J. S. Huang and B. T. Yen: Proof-tests of two slender-web welded plate girders. Fritz Engineering Laboratory Report: No. 327.7. 1969.
9) Fukumoto, Y. and I. Konishi: Local buckling of flanges in plate girders. Kansai Research Committee on Bridges, Steel Frames and Welding. 141-169. 1969.
10) Stein, M.: Loads and deformations of buckled rectangular plates. National Aeronautics and Space Administration Technical Report: No. R40. 1959.
11) Kawai, T.: Finite element analysis of the geometrically nonlinear problems of elastic plates. Recent Advances in Matrix Methods of Structural Analysis and Design. The University of Alabama Press, Alabama. 1971.
12) Hartz, B. J. and N. D. Nathan: Finite element formulation of geometrically nonlinear problems of elasticity. Recent Advances in Matrix Methods of Structural Analysis and Design. University of Alabama Press, Alabama. 1971.
13) Lang, T. E. and B. J. Hartz: Finite element matrix formulation of post-buckling stability and imperfection sensitivity. Proceedings of the Symposium of International Union of Theoretical and Applied Mechanics, held in Liège. 1970.
14) Kawamoto, T. and Y. Miyaike: A technique of material nonlinear finite element analysis. Proceedings of Japan Society of Civil Engineers 202: 25-32. 1972.
15) Kawamata, S., H. Ohyama, H. Nakaya and N. Tanaka: Problems of load incremental method in geometrically nonlinear problems. Proceedings of National Symposium on the Matrix Method for Structural Analysis and Design. Society of Steel Construction of Japan. 306-321. 1971.
16) Basler, K. and B. Thurliman: Strength of plate girders in bending. American Society of Civil Engineers Proceedings 87, No. ST6: 153-181. 1961.

NOTATION

a : length of panel
A : cross sectional area
b : depth of panel
C_s : scale factor for load-deflection curve
d_f : width of flange plate
D : flexural rigidity of plate
D_x, D_y: partial differential operators
E : modulus of elasticity
f : suffix denoting flange
G : modulus of rigidity
GJ: torsional rigidity
h : thickness of webplate
i : moment of inertia of cross section about the weak axis
I : moment of inertia of cross section about the strong axis
I_p : polar moment of inertia of cross section
k : ratio of elastic cross section
K, K' : equivalent torsional rigidity ratio
$\boldsymbol{K}, \boldsymbol{K}_0$: integro-differential operator
K_θ : spring constant
l : arc length of load-deflection curve segment
n, n_w, n_i, n_u, n_v: numbers of mesh points
N : dimension of mesh point system
p : $w^{(1)}/C_s$
q : $w^{(2)}/C_s$
t_f : thickness of flange
$\underline{u}, \underline{u}_0$: in-plane displacement vector
u, u_0 : in-plane displacement component in x-direction
v, v_0 : in-plane displacement component in y-direction
w, w^*, w_0, w_e, w_j: out-of-plane displacement component
x, y, z: coordinate system
α : σ_Y/E
β_f : d_f/t_f
γ : shearing strain
Δ : perturbation parameter
$\underline{\varepsilon}, \underline{\varepsilon}_0$: strain vector
ε_p : plastic axial strain
$\varepsilon_x, \varepsilon_y, \gamma_{xy}$: strain components
ζ_f : σ_r/σ_{Yf}
θ, θ_0 : angle of rotation of the compression flange
ν : Poisson's ratio
$\underline{\sigma}, \underline{\sigma}_0$: stress vector
$\sigma_x, \sigma_y, \tau_{xy}$: stress components
σ_r : residual stress
$\sigma_{Yf}, \sigma'_{Yf}$: yielding strength of flange
τ : shearing stress in the plane of webplate

APPENDIX A

Equations of Equilibrium of Webplates in Perturbed Form

The substitions of Eq. (13) into Eqs. (4) yield the following equations.

In-plane

$$\boldsymbol{RSR}^t\underline{u}^{(j)}+\boldsymbol{RS}(\boldsymbol{R}^t\boldsymbol{w}_0)(\boldsymbol{T}w^{(j)})$$
$$=-\frac{1}{2}\boldsymbol{RS}(\boldsymbol{R}^t\boldsymbol{w}^{(1)})(\boldsymbol{T}w^{(1)})\delta_{j2}\,, \quad \cdots\cdots\cdots\cdots(A\text{-}1)$$

where $j=1, 2$; δ_{j2} is a Kronecker's delta.

Out-of-plane

$$\frac{D}{h}\nabla^4 w^{(j)}=(\boldsymbol{T}^t\boldsymbol{R}w_0)\boldsymbol{S}\Big[R^t\underline{u}^{(j)}+(\boldsymbol{R}^t\boldsymbol{w}_0)(\boldsymbol{T}w^{(j)})$$
$$+\frac{1}{2}(\boldsymbol{R}^t\boldsymbol{w}^{(1)})(\boldsymbol{T}w^{(1)})\delta_{j2}\Big]$$
$$+(\boldsymbol{T}^t\boldsymbol{R}w^{(1)})\bar{\underline{e}}^{(1)}\delta_{j2}+(\boldsymbol{T}^t\boldsymbol{R}w^{(j)})\bar{\underline{e}}_0\,,$$
$$\cdots\cdots\cdots\cdots(A\text{-}2)$$

where

$$\bar{\underline{e}}^{(1)}=\boldsymbol{R}^t\underline{u}^{(1)}+(\boldsymbol{R}^t\boldsymbol{w}_0)(\boldsymbol{T}w^{(1)})\,.$$

Rigidities in Perturbed Form

The change of rigidities can be taken into account by using the similar expansions to Eq. (13). For instance, the equivalent torsional rigidity ratio of the compression flange, K, can be written in the form: (See Eq. (18))

$$K=k^{(0)}+\frac{1+\nu}{3\zeta_f}\log_e\frac{1}{1+\nu}[1+\nu+3\zeta_f(1-k^{(0)})]$$
$$+\frac{3}{2}\frac{(N-1)\zeta_f}{\alpha_f\zeta_f\beta[1+\nu+3\zeta_f(1-k^{(0)})]}(\tilde{u}^{(1)}_{\xi}\Delta+\tilde{u}^{(2)}_{\xi}\Delta^2)$$
$$-\frac{3}{8}\frac{(N-1)^2(1+\nu)}{[1+\nu+3\zeta_f(1-k^{(0)})]^2\alpha_f\beta^2\zeta_f}\tilde{u}^{(1)2}_{\xi}\Delta^2+0(\Delta^3)$$
$$\cdots\cdots\cdots\cdots(A\text{-}3)$$

where

$$k^{(0)}=\frac{1}{2\zeta_f}\left(1+\zeta_f+\frac{N-1}{\alpha\beta}\tilde{u}^{(0)}_{\xi}\right),$$

in which

$\alpha_f=\sigma_{Yf}/E$; $\beta=a/h$; $\xi=(N-1)x/a$; and $\tilde{u}=u/h$.

Similarly, the average stress of the compression flange in the elasto-plastic state can be expressed in the form:

$$\alpha_f=k^{(0)2}\zeta_f-1+\frac{k^{(0)}(N-1)}{\alpha_f\beta}(\tilde{u}^{(1)}_{\xi}\Delta+\tilde{u}^{(2)}_{\xi}\Delta^2)$$
$$+\frac{(N-1)^2}{4\alpha_f^2\zeta_f\beta^2}\tilde{u}^{(1)2}_{\xi}\Delta^2 \quad \cdots\cdots\cdots\cdots(A\text{-}4)$$

Then, the boundary conditions can also be written in the similar form. For instance, the first and second equations of Eq. (8) can be expressed in the following form:

$$\Big[\gamma_{fN}k^{(0)3}D_{\xi\xi\xi\xi}+12\frac{\alpha_f\beta^2\phi_f}{(N-1)}(1-\nu^2)(1-k^{(0)2}\zeta_f)D_{\xi\xi}-\frac{1}{\lambda^3}D_{\eta\eta\eta}-\frac{2-\nu}{\lambda}D_{\xi\xi\eta}\Big](\tilde{w}^{(1)}\Delta+\tilde{w}^{(2)}\Delta^2)$$
$$+\Big[\frac{3}{2}k^{(0)2}\frac{(N-1)}{\alpha_f\zeta_f\beta}\gamma_{fN}\tilde{w}^{(0)}_{\xi\xi\xi}-12(1-\nu^2)\beta\phi_f k^{(0)}\tilde{w}_{0,\xi\xi}\Big]D_{\xi}(\tilde{u}^{(1)}\Delta+\tilde{u}^{(2)}\Delta^2)$$
$$=-\frac{3}{4}k^{(0)}\frac{(N-1)^2}{\alpha_f^2\zeta_f^2\beta^2}\gamma_{fN}\tilde{w}^{(0)}_{\xi\xi\xi}\tilde{u}^{(1)2}_{\xi}\Delta^2+3(1-\nu^2)(N-1)\frac{\phi_f\beta}{\alpha_f\zeta_f}\tilde{u}^{(1)2}_{\xi}w_{0,\xi\xi}\Delta^2-\frac{3}{2}k^{(0)2}\frac{(N-1)}{\alpha_f\zeta_f\beta}\gamma_{fN}\tilde{w}^{(1)}_{\xi\xi\xi}\tilde{u}^{(1)2}_{\xi}\Delta^2$$
$$+12(1-\nu^2)\beta k^{(0)}\phi_f\tilde{w}^{(1)}_{\xi\xi}\tilde{u}^{(1)2}_{\xi}\Delta^2+0(\Delta^3)\,, \quad \cdots\cdots\cdots\cdots(A\text{-}5)$$

and, using Eq. (A-3),

$$\Big[\frac{\psi_{fN}}{\lambda}\Big\{k^{(0)}+\frac{1+\nu}{3\zeta_f}\log_e\frac{1}{1+\nu}[1+\nu+3\zeta_f(1-k^{(0)})]\Big\}D_{\xi\xi\eta}-\frac{\alpha_f\gamma_{fN}}{\lambda}\Big(1-\frac{1}{2}k^{(0)4}\zeta_f\Big)D_{\xi\xi\eta}+\frac{1}{\lambda^2}D_{\eta\eta}+\nu D_{\xi\xi}\Big]$$
$$\times(\tilde{w}^{(1)}\Delta+\tilde{w}^{(2)}\Delta^2)+\frac{(N-1)}{2\alpha_f\zeta_f\beta\lambda}\Big[\frac{3\psi_{fN}\zeta_f(1-k^{(0)})}{1+\nu+3\zeta_f(1-k^{(0)})}\tilde{w}^{(0)}_{\xi\xi\eta}+2\alpha_f\zeta_f\gamma_{fN}k^{(0)3}\tilde{w}_{0,\xi\xi\eta}\Big](\tilde{u}^{(1)}_{\xi}\Delta+\tilde{u}^{(2)}_{\xi}\Delta^2)$$
$$=\frac{3}{8}\frac{\psi_{fN}(N-1)^2(1+\nu)}{[1+\nu+3\zeta_f(1-k^{(0)})]^2}\frac{1}{\alpha_f\beta^2\lambda\zeta_f}\tilde{u}^{(1)2}_{\xi}\tilde{w}^{(0)}_{\xi\xi\eta}\Delta^2-\frac{3\gamma_{fN}k^{(0)2}(N-1)^2}{4\alpha_f\zeta_f\beta^2\lambda}\tilde{u}^{(1)2}_{\xi}\tilde{w}_{0,\xi\xi\eta}\Delta^2$$
$$-\Big[\frac{3\psi_{fN}\zeta_f(1-k^{(0)})(N-1)}{2\alpha_f\zeta_f\beta\lambda[1+\nu+3\zeta_f(1-k^{(0)})]}+k^{(0)3}\gamma_{fN}\frac{(N-1)}{\beta\lambda}\Big]\tilde{u}^{(1)}_{\xi}\tilde{w}^{(1)}_{\xi\eta}\Delta^2+0(\Delta^3)\,, \quad \cdots\cdots\cdots\cdots(A\text{-}6)$$

where

$\psi_{fN}=6(N-1)(1-\nu)[J_f/(ah^3)]$;

$\gamma_{fN}=12(1-\nu^2)(N-1)[I_f/(ah^3)]$;

and

$\phi_{fN}=A_f/(ah)$; $\lambda=b/a$; $\eta=(N-1)y/b$;

$\bar{w}=w/h$.

It will be seen that the change of rigidities can be simultaneously taken into account while the solution vectors $\underline{u}^{(1)}$ and $\underline{u}^{(2)}$ are sought.

APPENDIX B

Check of Convergence of Finite Differences

Whenever the finite difference method is used,

the convergence of solutions with respect to the number of mesh points must be examined to ensure the reliability of solutions.

In the present analysis, the convergence of the solutions may depend on the magnitude of the external load because of the nonlinear nature of the problem; as a necessary condition, however, good convergence of solutions is required at least at some small load level when the system performs almost linearly. For this reason, the following checks of convergence were performed.

In-plane Displacement

Panel C-1 This panel is subjected to both the shearing force and bending moment. The displacement component v can be identified as I_v $(=2N^2+5N-3)$th unknown in the mesh point system, and according to the simple beam theory, v can be obtained as:*

$$\frac{v}{h}=\frac{v_{SB}}{h}=\frac{\sigma_{Yw}ba^3}{3EI}\left(1+C\frac{b^2}{a^2}\right)\varepsilon;\quad \varepsilon=\tau/\sigma_{Yw}, \qquad \cdots\cdots\cdots\cdots\cdots\cdots\text{(B-1)}$$

where I refers to the moment of inertia of the cross section of the panel. From this equation, $v_{SB}/h=0.7824$ at $\varepsilon=0.1$. Table B-1 and Fig. B-1 show the values of the displacement component, v, corresponding to each value of N, and their relative differences. It is seen that the relative difference between the numerical result and the result from the simple beam theory is only 1.85% and 0.6% for $N=5$ and $N=7$, respectively.

Table B-1 Convergence of In-plane Displacement Component v
Panel C-1: $(w_0)_{max}/h=1.42$; No residual stresses; Load level: $\varepsilon=0.1$.

N	Total No. of Unknowns n	I_v	v/h	$\delta=v/h-v_{SB}/h$	$\frac{\delta}{v_{SB}/h}$
4	73	42	0.8047	+0.0223	+0.0285
5	109	72	0.9969	+0.0145	+0.0185
6	151	99	0.7892	+0.0068	+0.0087
7	199	130	0.7871	+0.0047	+0.0060

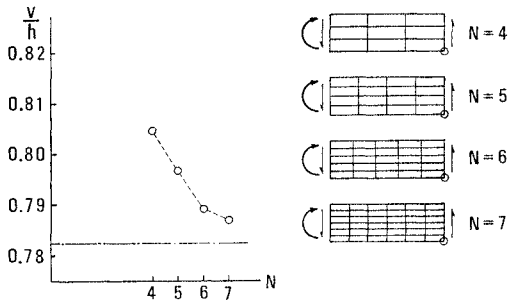

Fig. B-1 Convergence of Displacement Component v of Panel C-1.

* Parcel, J. I. and Moorman, R. B. B. Analysis of statically indeterminate structures. John Wiley & Sons, Inc., New York, 1955.

Panels M-1 and M-2 These panels are subjected to bending moment. The angle of rotation as shown in Fig. 18 can be predicted by the simple beam theory as:

$$\theta=\frac{\sigma_{Yw}a^2}{Eb^2}\frac{\varepsilon}{\frac{I}{ahb^2}};\quad \varepsilon=M/(\sigma_{Yw}ha^2). \qquad \cdots\cdots\cdots\cdots\cdots\cdots\text{(B-2)}$$

According to this equation, it is found that

$\theta=\theta_{SB}=0.0003819$ at $\varepsilon=0.1$ for Panel M-1,

and

$\theta=\theta_{SB}=0.0008403$ at $\varepsilon=0.1$ for Panel M-2.

Tables B-2 and B-3 show the values of the angle of rotation corresponding to each value of N, and their relative differences. It is seen from the result that the relative difference between the numerical result and the result from the simple beam theory is only 0.13% and 0.18% for $N=5$ and $N=7$, respectively for M-1; furthermore, 0.05% and 0.11% for $N=5$ and $N=7$, respectively for M-2.

Table B-2 Convergence of the Angle of Rotation θ
Panel M-1: $(w_0)_{max}/h=0.667$; No residual stresses; Load level: $\varepsilon=0.1$.

N	n	θ	$\delta=\theta-\theta_{SB}$	δ/θ_{SB}
4	73	0.0003872	+0.0000053	+0.0139
5	109	0.0003824	+0.0000005	+0.0013
6	151	0.0003936	+0.0000117	+0.0306
7	199	0.0003826	+0.0000007	+0.0018

Table B-3 Convergence of the Angle of Rotation θ
Panel M-2: $(w_0)_{max}/h=0.5$; No residual stresses; Load level: $\varepsilon=0.1$.

N	n	θ	$\delta=\theta-\theta_{SB}$	δ/θ_{SB}
4	73	0.0008635	+0.0000232	+0.0276
5	109	0.0008399	−0.0000004	−0.0005
6	151	0.0008697	+0.0000294	+0.0350
7	199	0.0008412	+0.0000009	+0.0011

(Received March 8, 1973)